

Theory of local heating in nanoscale conductors

Yu-Chang Chen, Michael Zwolak, and Massimiliano Di Ventra [*]

Department of Physics, Virginia Polytechnic Institute and State University, Blacksburg, Virginia 24061

We report first-principles calculations of local heating in nanoscale junctions formed by a single molecule and a gold point contact. Due to the lower current density and larger heat dissipation, the single molecule heats up less than the gold point contact. We also find that, at zero temperature, a threshold bias V_{onset} of about 6 mV and 11 mV for the molecule and the point contact, respectively, is required to excite the smallest vibrational mode and generate heat. The latter estimate is in very good agreement with recent experimental results on the same system. At a given external bias V below V_{onset} , heating becomes noticeable when the background temperature is on the order of $e(V_{\text{onset}} - V)/k_B$. Above V_{onset} , local heating increases dramatically with increasing bias but is also considerably suppressed by thermal dissipation into the electrodes. The results provide a microscopic picture of current-induced heat generation in atomic-scale structures.

Local heating occurs when electrons dissipating in a conductor release energy to the ions via scattering with phonons. The amount of heat generated in a given portion of the conductor depends on several factors: the strength of the electron-phonon interaction, the current density, the background temperature, and the electron mean free path. In a nanoscale junction, the electron mean free path is large compared to the dimensions of the junction. As a consequence, each electron releases only a small fraction of its energy during the time it spends in the junction. [1, 2, 3] However, there can still be substantial local heating due to the large current density in nanoscale junctions. Indeed, such an effect has recently been observed in several atomic-scale structures. [4, 5, 6] Apart from its fundamental importance in solid state physics, the problem has thus gained renewed interest due to its possible impact on nanoscale electronics. At this length scale, all atoms of the junction and corresponding vibrational modes need to be treated explicitly, and the electronic distribution calculated self-consistently with the correct scattering boundary conditions. Only a few theoretical investigations, mainly using the tight-binding approximation, have tackled this problem at the atomic level. [1, 2, 3]

In this letter, we derive a general expression for the power transferred by the electrons to the vibrational modes of a nanoscale junction and calculate the local heating using first-principles approaches. Combined with a model of heat transfer to the electrodes, the approach provides a microscopic and detailed picture of current-induced heat generation in nanoscale conductors. As an example, we discuss local heating for a single molecule between gold electrodes and a gold point contact. We find that the single-molecule junction heats up less than the gold point contact due to a larger heat dissipation into the electrodes and larger resistance to electron flow. In the case of the gold point contact, experimental data is available which is in very good agreement with the predicted threshold bias, V_{onset} , for heat generation and corresponding local temperature. At a given external bias V below V_{onset} , we find that local heating becomes noticeable when the background temperature is larger than

$e(V_{\text{onset}} - V)/k_B$, but is also considerably suppressed by thermal dissipation into the electrodes.

Let us start by considering a nanoscale structure between two bulk electrodes. The many-body Hamiltonian of the system is

$$H = H_{\text{el}} + H_{\text{ion}} + H_{\text{el-ion}}; \quad (1)$$

where H_{el} is the electronic Hamiltonian, $H_{\text{ion}} = \sum_{i=1}^N \frac{P_i^2}{2M_i} + \sum_{i < j} \frac{1}{2} V_{\text{ion}}(R_i - R_j)$ is the ionic Hamiltonian, and $H_{\text{el-ion}} = \sum_{i,j} V_{\text{el-ion}}(r_i - R_j)$ describes the electron-ion interaction. R_i , P_i , and M_i are the coordinates, momentum, and mass, respectively, of the i -th ion. r_i is the coordinate of the i -th electron. In the adiabatic approximation, the Hamiltonian (1) has effective single-particle eigenvalues $\epsilon_{\mathbf{k}}^{(L,R)}$ with energy E and momentum $\mathbf{K}_{\mathbf{k}}$ parallel to the electrode surface, corresponding to electrons incident from the left (right) electrodes. [7] We calculate the single-particle wavefunctions using a scattering approach within the density functional theory of many-electron systems. [7]

In order to calculate the electron-phonon interaction, we consider a small deviation $Q_i = R_i - R_i^0$ of the i -th ion from its equilibrium position R_i^0 . We introduce normal coordinates $q_{\mathbf{i}}$ such that the i -th component ($i = x, y, z$) of Q_i is

$$(Q_i)_{\mathbf{i}} = \sum_{j=1}^N \sum_{\mathbf{j}} A_{i,j} q_{\mathbf{j}}; \quad (2)$$

The transformation matrix, $A_p = f A_{i,j}$, satisfies the orthonormality relations: $\sum_i M_i A_{i,j} A_{i,j'} = \delta_{j,j'}$. The Hamiltonian describing the ionic vibrations can then be decoupled into a set of independent harmonic oscillators:

$$H_{\text{vib}} = \frac{1}{2} \sum_{i,j} \sum_{\mathbf{j}} q_{\mathbf{j}}^2 + \frac{1}{2} \sum_{i,j} \sum_{\mathbf{j}} f_{\mathbf{i}}^2 q_{\mathbf{j}}^2; \quad (3)$$

where $f_{\mathbf{i}}$ are the normal mode frequencies and the summations are carried out for all normal modes. We calculate these modes from first-principles. [8]

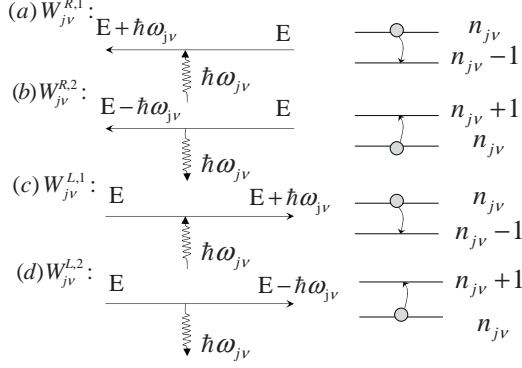


FIG. 1: Feynman diagrams of the four main electron-phonon scattering mechanisms contributing to local heating of the junction. (a) Cooling process due to absorption of a phonon from a left-moving electron. (b) Heating process due to the emission of a phonon from a left-moving electron. (c) and (d) are the equivalent mechanisms corresponding to the right-moving electrons.

We now introduce the field operator, $\hat{\psi} = \hat{\psi}^L + \hat{\psi}^R$, which describes electrons incident from the left (L) and right (R) electrodes, where [9]

$$\hat{\psi}^{L(R)} = \sum_E a_E^{L(R)} \psi_E^{L(R)}(\mathbf{r}; \mathbf{K}_k) \quad (4)$$

The coefficients $a_E^{L(R)}$ are the annihilation operators for electrons incident from the left (right) electrode. They satisfy the usual anti-commutation relations $\{a_E^i, a_{E'}^{j\dagger}\} = \delta_{ij} \delta_{EE'}$. We also assume that the electrons rapidly thermalize into the bulk electrodes so that their statistics are given by the equilibrium Fermi-Dirac distribution, $f_E^{L(R)} = 1/(\exp[(E - E_{FL(R)})/k_B T_e] + 1)$, in the left (right) electrodes, where T_e is the background temperature.

We can now express (Q_i) in terms of boson annihilation and creation operators. Together with the field operator $\hat{\psi}$, the second-quantized form of H_{vib} and the electron-vibration interaction, H_{el-vib} , can be written as

$$H_{vib} = \sum_{j=2}^N \left(\sum_{\mathbf{K}_k} \omega_{j\mathbf{K}_k} b_{j\mathbf{K}_k}^\dagger + \frac{1}{2} \right) \quad (5)$$

and

$$H_{el-vib} = \sum_{i,j} \sum_{\mathbf{K}_k} \sum_{\mathbf{K}_l} \frac{1}{2!} A_{i;j} J_{E_1 E_2}^{i;j} a_{E_1}^{\mathbf{K}_k} a_{E_2}^{\mathbf{K}_l} (b_{j\mathbf{K}_k}^\dagger + b_{j\mathbf{K}_k}) \quad (6)$$

where $i, j = L, R$; $i, j = 1, \dots, N$; and $\mathbf{K}_k = 1, 2, 3$. The quantity $J_{E_1 E_2}^{i;j}$ is the electron-vibration coupling

constant and has the form

$$J_{E_1 E_2}^{i;j} = \int d\mathbf{r} \int d\mathbf{K}_k \psi_{E_1}^i(\mathbf{r}; \mathbf{K}_k) \psi_{E_2}^j(\mathbf{r}; \mathbf{K}_k) V^{ps}(\mathbf{r}; \mathbf{R}_i) \quad (7)$$

where we have chosen to describe the electron-ion interaction with the pseudopotentials $V^{ps}(\mathbf{r}; \mathbf{R}_i)$ for each i -th ion. b_j are the annihilation operators for the j -th vibrational modes and satisfy the commutation relation $[b_j, b_{j'}^\dagger] = \delta_{jj'}$. The statistics of these modes are described by the Bose-Einstein distribution:

$$\langle b_j^\dagger b_{j'} \rangle = \delta_{jj'} \exp[-(n_j + 1/2)/k_B T_w] \quad (8)$$

where T_w is the local temperature of the junction.

For each normal mode, we can now calculate the rates of thermal energy generated by the electron-vibration interactions corresponding to the first-order processes described in Fig. 1. These processes correspond to electrons incident from the right or left electrode that absorb (cooling) or emit (heating) energy because of the electron-vibration scattering. We evaluate these rates with the Fermi golden rule

$$W_j^{R \rightarrow L} = 2 \pi \sum_{\mathbf{K}_k} \sum_{\mathbf{K}_l} \int dE \sum_i A_{i;j} J_{E E'}^{i;j} f_E^{L(R)} D_E^{L(R)} \quad (9)$$

$$W_j^{L \rightarrow R} = W_j^{R \rightarrow L}(R \leftrightarrow L); \quad (10)$$

where " $R \leftrightarrow L$ " means interchange of labels R and L; the positive (negative) sign in Eq. (9) is for $k = 1(2)$, corresponding to relaxation (excitation) of vibrational modes; $D_E^{L(R)}$ is the partial density of states corresponding to $\psi_E^{L(R)}$, whose sum is the total density of states. The term $\sum_{\mathbf{K}_k}$ corresponds to spontaneous emission. Finally, a factor of 2 due to spin degeneracy appears in Eq. (9).

Since electrons can excite all possible energy levels of a mode with frequency ω_j , the statistical average $\ln(n_j + 1)$ is required. The total thermal power generated in the junction is therefore the sum over all vibrational modes for the four processes of Fig. (1):

$$P = \sum_{j=2}^N (W_j^{R \rightarrow L} + W_j^{L \rightarrow R} + W_j^{R \rightarrow R} + W_j^{L \rightarrow L}) \quad (11)$$

Equation (11) is the central result of this paper. It allows for a first-principles calculation of the local temperature in a nanoscale junction. We now discuss results for two specific cases: local heating in a benzene-dithiolate molecular junction and a gold point contact (see schematics in Fig. 2). We also assume the left electrode to be positively biased. At zero temperature (i.e., $T_e = 0$ and $T_w = 0$), the heating processes $W_j^{L \rightarrow R}$, corresponding to electrons incident from the left electrode, vanish due

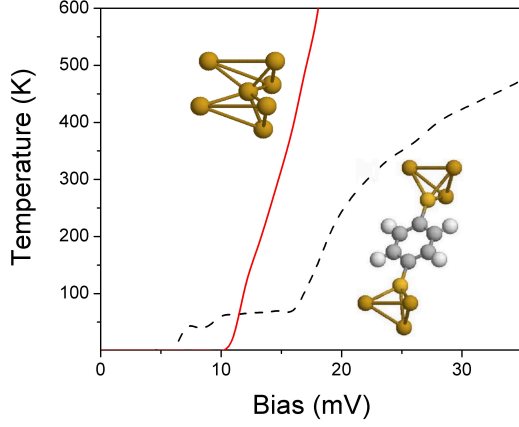


FIG. 2: Local equilibrium temperature as a function of bias for a benzene-dithiolate molecular junction (dashed line, schematic in the right-lower corner) and a single-gold-atom point contact (solid line, schematic in the left-upper corner) at $T_e = 0$ K. No heat dissipation into the electrodes is taken into account.

to the Pauli exclusion principle; the cooling processes $W_j^{R;1}$ and $W_j^{L;1}$, corresponding to the transitions from a high to a low energy level of the modes, are also prohibited because all modes are at the ground state. The only nonzero contribution to local heating is therefore from $W_j^{R;2}$, i.e.

$$P = 2 \sum_{j \in \text{vib}} \frac{X}{(1 + \ln(n_j + 1))} \sum_{i \in \text{vib}} \frac{X}{2} \frac{A_{i,j}}{E_{FL} + \epsilon_j} \frac{J_E^{i,LR}}{E_E - \epsilon_j} D_E^{L, \sim j} D_E^{R, \sim j} : \quad (12)$$

A bias greater than $V_{\text{onset}} = \min_j \epsilon_j$ is therefore necessary to generate heat. The smallest vibrational frequency calculated from first principles [8] is about 6 mV and 11 mV for the molecule and the point contact, respectively. The latter estimate is in very good agreement with recent experimental observations. [4] When the bias is smaller than the threshold voltage, local heating is only possible at nonzero background temperature T_e . This is caused by a small fraction of thermally excited electrons which can induce level transitions of the normal modes. The heating generated is substantial when $k_B T_e \sim \min_j \epsilon_j$ ($E_{FR} \sim E_{FL}$).

At $T_e = 0$ and $T_w > 0$, the junction heats up progressively, and eventually an equilibrium temperature is reached when the heating processes ($W_j^{R;2}$ and $W_j^{L;2}$) balance the cooling processes ($W_j^{R;1}$ and $W_j^{L;1}$). The corresponding local equilibrium temperature is plotted in Fig. 2 for both the single molecule junction and the

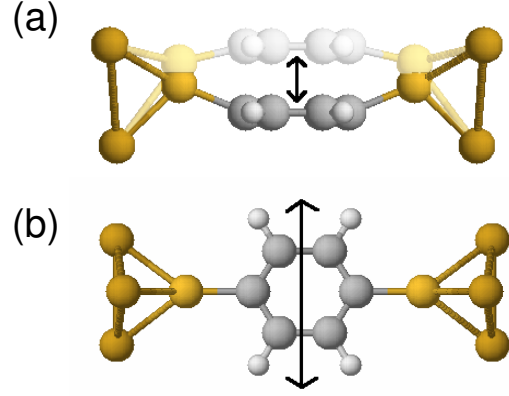


FIG. 3: The two modes contributing to heating at $T_e = 0$ and $V < 10$ mV. (a) The vibrational mode with energy ~ 6 meV. (b) The mode with energy ~ 9 meV.

gold point contact. It is evident from Fig. 2 that the equilibrium temperature increases abruptly above the threshold voltage and it is already substantial at biases of only few mV. The reason for this dramatic increase resides again in the Pauli exclusion principle which suppresses the cooling processes considerably.

In the case of the gold point contact, the longitudinal vibrational mode of the single gold atom (~ 11.5 meV) contributes the most to the local heating above $V = 11.5$ mV, even though the two transverse modes have slightly smaller frequencies (~ 10.8 meV) and are excited at a lower bias. In linear response ($V < 10$ mV), two modes contribute to local heating in the case of the single molecule junction (see Fig. 3). One, with energy ~ 6 meV, corresponds to the central benzene ring moving up and down with respect to its equilibrium position (Fig. 3(a)). The second, with energy ~ 9 meV, corresponds to the central ring moving sideways with respect to its equilibrium position (Fig. 3(b)). The first mode contributes to local heating almost three orders of magnitude more than the second one as determined by the transformation matrix $A_{i,j}$. At a bias of about 0.5V, all vibrational modes of the molecular junction are excited. The mode that contributes the most to the heating corresponds to an in-plane "breathing" of the central carbon ring (not shown). [10]

So far we have assumed the junction is thermally isolated. However, the majority of the heat generated in the junction is actually transferred to the electrodes. We estimate the thermal conductance following the approach of Patton and Geller. [11] We assume the junction to be a weak thermal link with a given stiffness K , which we evaluate from first principles. [12] We then estimate the thermal current into the electrodes via elastic phonon

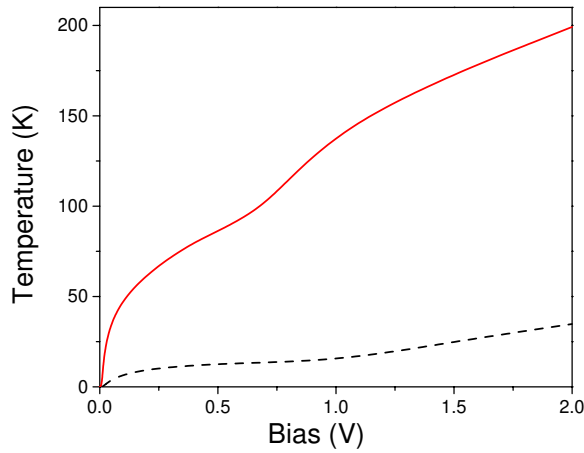


FIG. 4: Local temperature as a function of bias for a benzene-dithiolate molecular junction (dashed line) and a gold point contact (solid line) due to the equilibrium between local heating and heat dissipation into the electrodes at $T_e = 0$ K.

scattering as [11]

$$I_{th} = \frac{4 K^2 Z}{\pi} \int d\omega N_L(\omega) N_R(\omega) [n_L(\omega) - n_R(\omega)]; \quad (13)$$

where $n_{L(R)}$ is the Bose-Einstein distribution function, $N_{L(R)}(\omega)$ is the spectral density of states at the left (right) electrode surface, and $K = d^2 Y / (4l)$. Y is the Young's modulus of the junction, and d (l) is its diameter (length). [11] We note that the temperature profile along a nanojunction is nearly constant and almost equal to the average temperature of the thermal reservoirs. [13, 14, 15, 16] The thermal current from the junction with temperature T_w dissipated to the left electrode with temperature T_e is thus equivalent to the thermal current of a weak thermal link between reservoirs with temperatures T_e and $2T_w - T_e$. Analogously for the thermal current into the right electrode. The effective local temperature, resulting from the equilibrium between local heating and heat dissipation into the electrodes, is plotted in Fig. 4 at $T_e = 0$ K. Values of the local temperature for the gold contact are in good agreement with experimental results [6] and previous theoretical estimates. [1] It is evident from Fig. 4 that the local temperature is considerably reduced by heat transfer into the electrodes even for relatively large biases (cf. Fig. 2). It is also evident that at any given bias the single-molecule junction heats up less than the gold point contact. This is due to the larger stiffness of the molecule and its larger

resistance to electrical current.

We thank T. N. Todorov for useful discussions. We acknowledge support from the NSF Grant Nos. DMR-01-02277 and DMR-01-33075, and Carilion Biomedical Institute. Acknowledgment is also made to the Donors of The Petroleum Research Fund, administered by the American Chemical Society, for partial support of this research.

* Corresponding author. E-mail address: diventra@vt.edu.

¹ T. N. Todorov, Phil. Mag. B 77, 965 (1998).

² M. J. Montgomery, T. N. Todorov, and A. P. Sutton, J. Phys.: Cond. Mat. 14, 1 (2002).

³ M. J. Montgomery, J. Hoekstra, T. N. Todorov, and A. P. Sutton, J. Phys.: Cond. Mat. (in press).

⁴ N. Agrat, C. Untiedt, G. Rubio-Bollinger, and S. Vieira, Phys. Rev. Lett. 88, 216803 (2002).

⁵ C. J. Muller, J. M. van Ruitenbeek, and J. L. Jongh, Phys. Rev. Lett. 69, 140 (1992).

⁶ H. E. van den Brom, A. J. Yanson, and J. M. van Ruitenbeek, Physica B 252, 69 (1998).

⁷ N. D. Lang, Phys. Rev. B 52, 5335 (1995); M. DiVentra and N. D. Lang, Phys. Rev. B 65, 045402 (2002); Z. Yang, A. Tackett, and M. DiVentra, Phys. Rev. B 66, 041405 (2002); M. DiVentra, S. T. Pantelides, and N. D. Lang, Phys. Rev. Lett. 84, 979 (2000).

⁸ We have employed Hartree-Fock total energy calculations [see, e.g., J. A. Boatz and M. S. Gordon, J. Phys. Chem. 93, 1819 (1989)] to evaluate the vibrational modes of the single-molecule junction and the gold point contact. For these calculations, the gold electrodes have been represented by a triangular pad of gold atoms (see insets of Fig. 2) within finite mass.

⁹ Y.-C. Chen and M. DiVentra, cond-mat/0208066.

¹⁰ M. DiVentra, S. T. Pantelides, and N. D. Lang, Phys. Rev. Lett. 88, 046801 (2002).

¹¹ K. R. Patton and M. R. Geller, Phys. Rev. B 64, 155320 (2001).

¹² The following parameters have been used: Young modulus of the gold contact, 5.0×10^{11} dyne/cm² [from B. K. Rakhe and B. Damaschke, Appl. Phys. Lett. 77, 361 (2000)]; Young modulus of the benzene-dithiolate molecule, 52.6×10^{11} dyne/cm² (estimated from total energy calculations); gold effective diameter, 4.6 a.u.; sulfur effective diameter 6.9 a.u. The spectral densities $N_{L(R)}(\omega)$ are estimated according to Ref. [11], with longitudinal and transverse sound velocities for bulk gold, $v_l = 3.2 \times 10^8$ cm/sec and $v_t = 1.2 \times 10^8$ cm/sec, respectively.

¹³ U. Zücher and P. Talkner, Phys. Rev. A 42, 3278 (1990).

¹⁴ A. Dhar, Phys. Rev. Lett. 86, 5882 (2001); cond-mat/0210470

¹⁵ A. Ozpineci and S. Ciraci, Phys. Rev. B 63, 125415 (2001).

¹⁶ K. Saito, S. Takesue, and S. Miyashita, Phys. Rev. E 61, 2397 (2000).